Difference-Frequency MUSIC for DOAs

Yongsung Park, *Member, IEEE*, Peter Gerstoft, *Fellow, IEEE*, and Jeung-Hoon Lee

***Abstract*—The direction-of-arrivals (DOAs) of plane waves in a high-frequency region are estimated without spatial aliasing using multi-frequency processing. The method exploits the difference frequency (DF), the difference between two high frequencies. This enables processing data in a feasible region without spatial aliasing. We analyze DOA characteristics upon DF processing and propose a MUSIC-based method dealing with multi-DF and multi-snapshot. Multiple DFs having the same frequency difference allow processing multi-DF equivalently to multi-snapshot. We propose a method that considers all DFs and snapshots jointly and a joint DF method providing a single snapshot DF-MUSIC that does not require stationary DOAs. Numerical examples validate the effectiveness of the proposed method and its DOA performance is discussed.**

***Index Terms*—Array signal processing, direction of arrival (DOA) estimation, wideband sources, difference frequency.**

I. Introduction

DUE to spatial aliasing, uniform linear arrays limit the plane-wave DOA estimation to an upper frequency. To consider a specific frequency component of data, data should be sampled at more than two points per wavelength. Otherwise, the DOA becomes ambiguous with components at wrong DOAs. This problem arises especially with passive systems when processing out-of-band signals at higher frequencies.

We solve the high-frequency DOA estimation and employ multi-frequency processing. More data from multiple frequencies in a wideband signal achieves the processing gain and obtains good estimates [1], [2], [3], [4]. For better wideband DOA estimation, sparse signal reconstruction has been proposed [5], [6], [7], [8], [9], [10]. The cyclo-stationarity-based wideband method is another technique and utilizes cyclic correlation property in time and space [11], [12], [13], [14], [15]. The spectral property of multi-frequency has been used to improve DOA estimation for the co-prime array, a famous non-uniform linear array [16], [17], [18], [19]. The method uses multiple frequencies to fill the missing virtual co-array elements.

The multi-frequency processing exploits the difference frequency (DF), the product of array data at frequency f with the complex conjugate at another $f + \Delta f$, which enables dealing with data in the lower frequency Δf region without spatial aliasing [20], [21]. The DOA estimation of far-field sources has the array data model with a sum of plane waves.

The DF technique has been applied for source localization and DOA estimation and validated with experimental data [21], [22], [23], [24]. For source localization, matched field processing which matches measured and simulated signals using wave propagation models have been applied [25], [26], [27], [28]. For DOA estimation, a conventional beamformer (CBF) or a delay-and-sum beamformer was used [21]. DF method using high frequencies has shown comparable DOA performance to CBF at low-frequency [22]. Improved DOA performance of the DF-based CBF by deconvolution [23] and by using the MVDR and further analytic considerations [24]. As shown here, the DF processing uses the Hadamard product of array data at frequency f and the complex conjugate data at $f + \Delta f$.

DF processing is here using the MUSIC subspace-based beamformer, which achieves higher DOA resolution compared to CBF on DF-data. We propose three ways to combine multiple time and DF samples: time, frequency, and time-frequency.

The time-DF-MUSIC use multiple time samples for a single DF to obtain a time-averaged sample covariance matrix (SCM). Utilizing DFs gives unwanted artifact DOAs [21], [22], [24], which depend on the true DOAs and the DF frequencies. As the artifact DOAs vary across DFs, obtaining MUSIC spectra for each DF separately and averaging across frequency mitigates the artifacts.

The frequency-DF-MUSIC use uniformly-spaced multi-DFs, having the same DF to obtain a frequency-averaged SCM. The constant DFs share the same steering vectors for true DOAs, and the multi-DF is used equivalently to multi-snapshot. The frequency processing uses multiple DFs, and we achieve single-time snapshot DOA estimation. The single time-snapshot method is useful for time-varying DOAs.

The time-frequency DF-MUSIC combine all time and DF samples into a SCM. The method improves DOA estimation using more data averaging.

The method is flexible, e.g., root-MUSIC [29] for gridless processing [30], [31], [32], [33], [34] is possible. Extensions are applicable, such as 2D DOA estimation [35], [36], [37] and 3D source localization [38], [39], [40]. Aliasing can be avoided with the DF processing for nonuniform linear arrays [41], [42], [43], [44], including co-prime arrays [45], [46], or multi-dimensional arrays [47], [48].

Notation: For a matrix $\mathbf{A}$, $\mathbf{A}^{\mathsf{T}}$ is the transpose, $\mathbf{A}^*$ is the complex conjugate, and $\mathbf{A}^{\mathsf{H}}$ is the conjugate transpose. The Hadamard products of matrices $\mathbf{A}$ and $\mathbf{B}$ is denoted $\mathbf{A} \circ \mathbf{B}$.

II. Array Data Model

Consider K DOAs with L snapshots at frequency f. We assume the sources with DOAs $\theta_k \in [-90^\circ, 90^\circ)$ are in the far-field of a uniform linear array (ULA) with M sensors. Let

Manuscript received 29 July 2022; revised 13 December 2022; accepted 13 December 2022. Date of publication 19 December 2022; date of current version 26 December 2022. This work was supported in part by the Office of Naval Research under Grant N00014-21-1-2267 and in part by the National Research Foundation of Korea under Grant 2021R1A2C1005962. The associate editor coordinating the review of this manuscript and approving it for publication was Dr. Jean Pierre Delmas. *(Corresponding author: Yongsung Park.)*

Yongsung Park and Peter Gerstoft are with the NoiseLab at the Scripps Institution of Oceanography, University of California San Diego, La Jolla, CA 92093 USA (e-mail: yongsungpark@ucsd.edu; gerstoft@ucsd.edu).

Jeung-Hoon Lee is with the School of Mechanical Engineering, Changwon National University, Uichang-gu, Changwon 51140, South Korea (e-mail: jhoonlee@changwon.ac.kr).

Digital Object Identifier 10.1109/LSP.2022.3230365

$\mathbf{X}_f = [\mathbf{x}_{t_1,f} \dots \mathbf{x}_{t_L,f}] \in \mathbb{C}^{K\times L}$ be the complex source amplitudes, $x_{kt_l,f}$ with $k \in [1 \dots K]$ and $l \in [1 \dots L]$, and the array data $\mathbf{Y}_f = [\mathbf{y}_{t_1,f} \dots \mathbf{y}_{t_L,f}] \in \mathbb{C}^{M\times L}$ is modeled as

$$\mathbf{Y}_f = \sum_{k=1}^{K} \mathbf{a}_f(\theta_k)\mathbf{x}_{k,f}^{\mathsf{T}} + \mathbf{E}_f, \tag{1}$$

where $\mathbf{x}_{k,f} = [x_{kt_1,f} \dots x_{kt_L,f}]^{\mathsf{T}} \in \mathbb{C}^L$, $\mathbf{E}_f \in \mathbb{C}^{M\times L}$ is the additive noise, and the steering vector,

$$\mathbf{a}_f(\theta) = \left[e^{-j2\pi f d_1 \sin\theta/c} \dots e^{-j2\pi f d_M \sin\theta/c}\right]^{\mathsf{T}} \in \mathbb{C}^M, \tag{2}$$

where c is the sound speed and $[d_1 \dots d_M] = [0 : M-1]$ is the ULA element spacing. The additive noise $\mathbf{E}_f$ is assumed independent across sensors and snapshots, with each element following a complex Gaussian $\mathcal{CN}(0,\sigma^2)$.

III. Difference Frequency DOA Estimation

A. Hadamard Product for Difference Frequency

We model the array data for a single frequency as a sum of plane waves (1) and assume multi-frequencies arrive at the array at the same DOAs. To exploit the frequency difference, $\Delta f_i = f_i' - f_i$, $f_i' > f_i$, we utilize the Hadamard product of frequency data $\mathbf{Y}_{f_i'}$ and the complex conjugate of frequency data $\mathbf{Y}_{f_i}$, giving $\mathbf{Z}_{\Delta f_i} \in \mathbb{C}^{M\times L}$,

$$\begin{aligned}\mathbf{Z}_{\Delta f_i} &= \mathbf{Y}_{f_i'} \circ \mathbf{Y}_{f_i}^* = [\mathbf{y}_{t_1,f_i'} \dots \mathbf{y}_{t_L,f_i'}] \circ [\mathbf{y}_{t_1,f_i}^* \dots \mathbf{y}_{t_L,f_i}^*] \\ &= \sum_{k=1}^{K} \mathbf{a}_{\Delta f_i}(\theta_k)\left[\mathbf{x}_{k,f_i'}^{\mathsf{T}} \circ \mathbf{x}_{k,f_i}^{\mathsf{H}}\right] \\ &\quad + \sum_{\substack{k'=1\\k'\neq k''}}^{K}\sum_{k''=1}^{K}\left[\mathbf{a}_{f_i'}(\theta_{k'}) \circ \mathbf{a}_{f_i}^*(\theta_{k''})\right]\left[\mathbf{x}_{k,'f_i'}^{\mathsf{T}} \circ \mathbf{x}_{k,''f_i}^{\mathsf{H}}\right] + \mathbf{E}_\Delta,\end{aligned} \tag{3}$$

$$\begin{aligned}\mathbf{a}_{\Delta f_i}(\theta) &= \mathbf{a}_{f_i'}(\theta) \circ \mathbf{a}_{f_i}^*(\theta) \\ &= \left[e^{-j2\pi\Delta f_i d_1 \sin\theta/c} \dots e^{-j2\pi\Delta f_i d_M \sin\theta/c}\right]^{\mathsf{T}}.\end{aligned} \tag{4}$$

Compared to (1), the product $\mathbf{Z}_{\Delta f_i}$ (3) is a sum of steering vectors but in Δf_i, $\mathbf{a}_{\Delta f_i}(\theta)$ (4). Unlike the frequencies $\{f_i', f_i\}$, the DF Δf_i is below array aliasing frequency.

However, as the processing frequency is lowered, $\Delta f_i < f_i$, the resolution of the beamformer deteriorates. Conventional beamforming gets the beamwidth of the main lobe increased, and this decreases the resolution. Also, the cross-terms in (3) show unwanted artifact DOA patterns in the beamforming spectrum. K true DOAs have $K^2 - K$ artifact DOAs, determined by the frequency and true DOAs.

The artifact DOAs $\tilde{\theta}$ vary based on frequencies $\{f_i, f_i'\}$ and true DOAs θ_k. They can be found by assuming the power $\mathbf{x}_{k,f_i} = \mathbf{x}_{k,f_i'} = \mathbf{1}$, only retaining the cross terms in (3), and finding when the beam power is 1,

$$\mathbf{a}_{\Delta f_i}(\tilde{\theta})^{\mathsf{T}}\left[\sum_{\substack{k'=1\\k'\neq k''}}^{K}\sum_{k''=1}^{K}\mathbf{a}_{f_i'}(\theta_{k'}) \circ \mathbf{a}_{f_i}^*(\theta_{k''})\right] = 1. \tag{5}$$

Solving this gives the artifact DOAs $\tilde{\theta}$

$$\tilde{\theta} = \sin^{-1}\left(\frac{f_i' \sin\theta_{k'} - f_i \sin\theta_{k''}}{f_i' - f_i}\right),\ k' \neq k''. \tag{6}$$

We will propose methods to deal with the artifact DOAs. A method obtains multiple beamforming spectra using single DFs and averages them. Then, the artifact DOAs varying across DFs mitigate. Another method combines multi-DF data jointly into a SCM and estimates DOAs. Both thus need multiple DF data.

B. DF-CBF

DF DOA estimation uses the product $\mathbf{Z}_{\Delta f_i}$ (3) and the steering matrix using $\mathbf{a}_{\Delta f_i}(\theta)$ (4). The CBF for DF DOA estimation uses the DF-SCM $\mathbf{R}_{\text{DF}}$. For N potential DOAs $\bar{\boldsymbol{\theta}} = [\bar{\theta}_1 \dots \bar{\theta}_N]^{\mathsf{T}} \in [-90^\circ, 90^\circ)$, the DF-CBF power is then,

$$P_{\Delta f_i}^{\text{DF-CBF}}(\bar{\theta}_n) = \mathbf{a}_{\Delta f_i}^{\mathsf{H}}(\bar{\theta}_n)\mathbf{R}_{\text{DF}}\mathbf{a}_{\Delta f_i}(\bar{\theta}_n), \tag{7}$$

$$\begin{aligned}\mathbf{R}_{\text{DF}} &= \frac{1}{L}\sum_{l=1}^{L}\mathbf{z}_{t_l,\Delta f_i}\mathbf{z}_{t_l,\Delta f_i}^{\mathsf{H}} \\ &= \frac{1}{L}\sum_{l=1}^{L}\left(\mathbf{y}_{t_l,f_i'}\mathbf{y}_{t_l,f_i'}^{\mathsf{H}}\right) \circ \left(\mathbf{y}_{t_l,f_i}\mathbf{y}_{t_l,f_i}^{\mathsf{H}}\right)^*.\end{aligned} \tag{8}$$

Note that CBF for a single frequency f uses $\mathbf{Y}_f$ (1), $\mathbf{a}_f(\theta)$ (2), and the data SCM, i.e., $\sum_{l=1}^{L}\mathbf{y}_{t_l,f}\mathbf{y}_{t_l,f}^{\mathsf{H}}/L$. DF processing uses the Hadamard product of two array covariance matrices (8).

IV. DF-MUSIC With Time and Frequency Samples

We propose three ways to consider L-time and F-DF samples. The time-DF-MUSIC treats each DF separately (12b). We then compute F independent MUSIC spectra and average these. Assuming the DF constant, the frequency-DF-MUSIC treats each time sample separately and combines only frequency samples into a DF-SCM (13b), and time-averages the L MUSIC spectra. The time-frequency-DF-MUSIC treats all LF time and frequency jointly into one DF-SCM (14b).

A. Multiple Time and DF Samples

For F-DFs, $\Delta f_i = f_i' - f_i$, $i = 1, \dots, F$ and L-snapshots, we have LF-number of measurements. Let us recall a single vector $[\mathbf{Z}_{\Delta f_i}]_{:,l}$ (3) and re-express it as $\mathbf{z}_s = [z_1^{(s)} \dots z_M^{(s)}]^{\mathsf{T}}$, $s \in \mathcal{S} = \{t_1, \dots, t_L\} \times \{\Delta f_1, \dots, \Delta f_F\}$. The sth observation among multiple samples is, assuming s corresponds to $(t_l, \Delta f_i)$,

$$\begin{aligned}\mathbf{z}_s &= \sum_{k=1}^{K} x_{kt_l,f_i'}x_{kt_l,f_i}^*\mathbf{a}_{\Delta f}(\theta_k) \\ &\quad + \sum_{\substack{k'=1\\k'\neq k''}}^{K}\sum_{k''=1}^{K} x_{k't_l,f_i'}x_{k''t_l,f_i}^*\left[\mathbf{a}_{f_i'}(\theta_{k'}) \circ \mathbf{a}_{f_i}^*(\theta_{k''})\right] + \mathbf{e}_\Delta \\ &= \left[\sum_{k=1}^{K}\tilde{x}_k^{(s)}[\mathbf{a}_{\Delta f_i}(\theta_k)]_1 \dots \sum_{k=1}^{K}\tilde{x}_k^{(s)}[\mathbf{a}_{\Delta f_i}(\theta_k)]_M\right]^{\mathsf{T}} + \mathbf{e}_c + \mathbf{e}_\Delta,\end{aligned} \tag{9}$$

where $\mathbf{e}_c$ is the cross-term and $\mathbf{e}_\Delta$ is the noise for $[\mathbf{Z}_{\Delta f_i}]_{:,l}$ (3).

Assuming $\tilde{x}_k^{(s)}$, $\mathbf{e}_c$, and $\mathbf{e}_\Delta$ are uncorrelated, the DF-covariance matrix is

$$\mathbf{R} = \mathbb{E}\{\mathbf{z}_s \mathbf{z}_s^{\mathsf{H}}\} = \mathbf{A}\mathbf{R}_{\tilde{x}}\mathbf{A}^{\mathsf{H}} + \mathbf{R}_c + \mathbf{R}_\Delta, \tag{10}$$

where $\mathbf{A} = [\mathbf{a}_{\Delta f_i}(\theta_1) \dots \mathbf{a}_{\Delta f_i}(\theta_K)] \in \mathbb{C}^{M\times K}$ and $\mathbf{R}_{\tilde{x}}$ is the amplitude covariance matrix whose elements are $[\mathbf{R}_{\tilde{x}}]_{i,j} = \mathbb{E}\{\tilde{x}_i^{(s)} \tilde{x}_j^{*(s)}\}$. The DF-covariance matrix composed of $|\mathcal{S}|$ samples provides joint processing over the multiple samples. We consider an estimated covariance matrix, DF-SCM,

$$\hat{\mathbf{R}} = \frac{1}{|\mathcal{S}|}\sum_{s=1}^{|\mathcal{S}|} \mathbf{z}_s \mathbf{z}_s^{\mathsf{H}}. \tag{11}$$

The estimate (11) converges to (10) for $|\mathcal{S}| \to \infty$ in a mean square sense [49]. Given F DFs $\Delta f_1, \dots, \Delta f_F$ and L snapshots $t_1, \dots, t_L$, LF products $\mathbf{z}_{t_l,\Delta f_i}$ are available. We combine $\mathbf{z}_{t_l,\Delta f_i}$ to obtain

1) time-averaged DF-SCM

$$\mathbf{Z}_{L,\Delta f_i} = [\mathbf{z}_{t_1,\Delta f_i} \dots \mathbf{z}_{t_L,\Delta f_i}], \qquad i = 1, \dots, F, \tag{12a}$$

$$\mathbf{R}^{\text{time}}_{\text{DF},\Delta f_i} = \mathbf{Z}_{L,\Delta f_i}\mathbf{Z}^{\mathsf{H}}_{L,\Delta f_i}/L, \tag{12b}$$

2) frequency (DF) averaged SCM

$$\mathbf{Z}_{t_l,F} = [\mathbf{z}_{t_l,\Delta f_1} \dots \mathbf{z}_{t_l,\Delta f_F}], \qquad l = 1, \dots, L, \tag{13a}$$

$$\mathbf{R}^{\text{frequency}}_{\text{DF},t_l} = \mathbf{Z}_{t_l,F}\mathbf{Z}^{\mathsf{H}}_{t_l,F}/F, \tag{13b}$$

3) time-and-frequency avearaged SCM

$$\mathbf{Z}^{\text{time-frequency}}_{\Delta f} = [\mathbf{z}_{t_1,\Delta f_1} \dots \mathbf{z}_{t_L,\Delta f_1} \dots \mathbf{z}_{t_1,\Delta f_F} \dots \mathbf{z}_{t_L,\Delta f_F}], \tag{14a}$$

$$\mathbf{R}^{\text{time-frequency}}_{\text{DF}} = \mathbf{Z}^{\text{time-frequency}}_{\Delta f}\mathbf{Z}^{\text{time-frequency}\,\mathsf{H}}_{\Delta f}/(LF). \tag{14b}$$

B. DF-MUSIC

DF-MUSIC is a subspace method. It eigendecomposes the DF-SCM $\mathbf{R}_{\text{DF}} \in \mathbb{C}^{M\times M}$ (12b,13b,14b) into signals and noise,

$$\mathbf{R}_{\text{DF}} = \mathbf{U}_{\text{signal}}\mathbf{\Lambda}_{\text{signal}}\mathbf{U}^{\mathsf{H}}_{\text{signal}} + \mathbf{U}_{\text{noise}}\mathbf{\Lambda}_{\text{noise}}\mathbf{U}^{\mathsf{H}}_{\text{noise}}. \tag{15}$$

The eigenvectors corresponding to the K^2 largest eigenvalues $\mathbf{U}_{\text{signal}}$ span a signal subspace (there are still noise components in the signal subspace). Due to the cross terms (3), there are upto K^2 eigenvalues above the noise floor, not K. The remaining $M - K^2$ eigenvectors $\mathbf{U}_{\text{noise}}$ span a noise subspace, which does not have signal components and is orthogonal to the signal subspace,

$$\mathbf{U}^{\mathsf{H}}_{\text{noise}}\mathbf{a}_{\Delta f}(\theta_k) = \mathbf{0}, \quad k = 1, \dots, K^2. \tag{16}$$

DOAs θ_k are estimated from the DF-MUSIC power,

$$P^{\text{DF-MUSIC}}(\bar{\theta}_n) = \left[\mathbf{a}^{\mathsf{H}}_{\Delta f}(\bar{\theta}_n)\mathbf{U}_{\text{noise}}\mathbf{U}^{\mathsf{H}}_{\text{noise}}\mathbf{a}_{\Delta f}(\bar{\theta}_n)\right]^{-1}. \tag{17}$$

C. Time-DF-MUSIC

Joint-time processing performs DF-MUSIC (17) F-times with $\mathbf{Z}_{L,\Delta f_i} \in \mathbb{C}^{M\times L}$ (12a), i.e., $\mathbf{R}_{\text{DF}} = \mathbf{R}^{\text{time}}_{\text{DF},\Delta f_i}$, and averages F MUSIC spectra $\{P^{\text{DF-MUSIC}}\big|_{\Delta f_1} \dots P^{\text{DF-MUSIC}}\big|_{\Delta f_F}\}$,

$$P^{\text{time}}_{\text{DF-MUSIC}}(\bar{\theta}_n) = \frac{1}{F}\sum_{i=1}^{F} P^{\text{DF-MUSIC}}(\bar{\theta}_n)\big|_{\Delta f_i}. \tag{18}$$

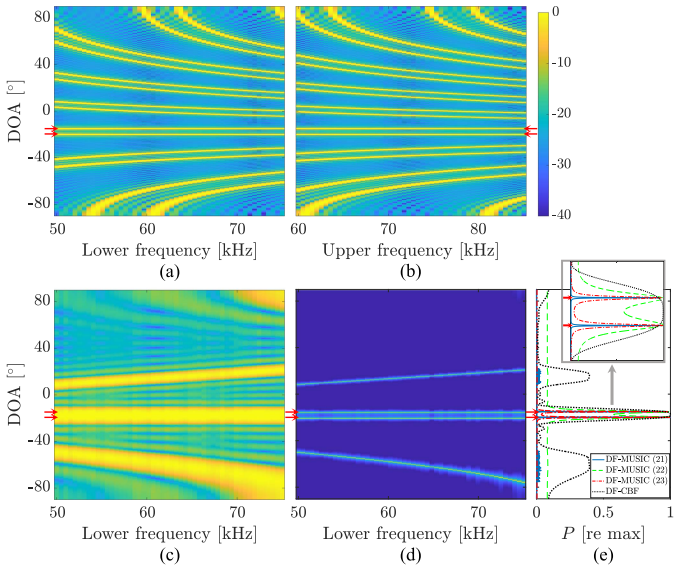

Fig. 1. CBF versus frequencies for the (a) lower and (b) upper frequencies, used for the DFs. DF-DOA estimation versus DFs: (c) DF-CBF (7) and (d) DF-MUSIC (17). (e) Spectra averaged over DFs: DF-CBF (dotted), time-(18) (solid), frequency-(19) (dashed), and time-frequency-DF-MUSIC (20) (dash-dot). Power is normalized with maximum. DOAs are at $[-20, -15]^\circ$ ($\rightarrow$).

Averaging over F DFs mitigates artifacts from the cross-terms in (3), see Fig. 1.

D. Frequency-DF-MUSIC

Joint-frequency processing performs DF-MUSIC (17) L-times with $\mathbf{Z}_{t_l,F} \in \mathbb{C}^{M\times F}$ (13a), i.e., $\mathbf{R}_{\text{DF}} = \mathbf{R}^{\text{frequency}}_{\text{DF},t_l}$, and averages L MUSIC spectra $\{P^{\text{DF-MUSIC}}\big|_{t_1} \dots P^{\text{DF-MUSIC}}\big|_{t_L}\}$,

$$P^{\text{frequency}}_{\text{DF-MUSIC}}(\bar{\theta}_n) = \frac{1}{L}\sum_{l=1}^{L} P^{\text{DF-MUSIC}}(\bar{\theta}_n)\big|_{t_l}. \tag{19}$$

Note that, each MUSIC spectrum $P^{\text{DF-MUSIC}}\big|_{t_l}$ corresponds to a single snapshot performance of DF-MUSIC.

E. Time-Frequency-DF-MUSIC

Joint-time-frequency processing performs DF-MUSIC (17) with $\mathbf{Z}^{\text{time-frequency}}_{\Delta f} \in \mathbb{C}^{M\times LF}$ (14a), i.e., $\mathbf{R}_{\text{DF}} = \mathbf{R}^{\text{time-frequency}}_{\text{DF}}$,

$$P^{\text{time-frequency}}_{\text{DF-MUSIC}}(\bar{\theta}_n) = P^{\text{DF-MUSIC}}(\bar{\theta}_n). \tag{20}$$

Remark (Uniform DFs and joint-frequency processing): The frequency- and time-frequency-DF-MUSIC require uniformly-spaced DFs, i.e., $\Delta f_i = \Delta f$, $i = 1, \dots, F$. Let us recall the product $\mathbf{Z}_{L,\Delta f_i} \in \mathbb{C}^{M\times L}$ (12a). Note that, L time samples are concatenated as each $\mathbf{z}_{t_l,\Delta f_i}$ shares the same DF-steering vectors $\mathbf{a}_{\Delta f_i}(\theta)$ (4) over L snapshots.

For the constant DF $\Delta f_i = \Delta f$, the DF-steering vector $\mathbf{a}_{\Delta f_i}(\theta)$ (4) is the same over F DF pairs, i.e.,

$$\mathbf{a}_{\Delta f}(\theta) = \mathbf{a}_{\Delta f_1}(\theta) = \dots = \mathbf{a}_{\Delta f_F}(\theta). \tag{21}$$

This provides that $\mathbf{z}_{t_l,\Delta f_i}$, $i = 1, \dots, F$, shares the same $\mathbf{a}_{\Delta f}(\theta)$ (21). We concatenate F DF samples, e.g., $\mathbf{Z}_{t_l,F} \in \mathbb{C}^{M\times F}$ (13a) and $\mathbf{Z}^{\text{time-frequency}}_{\Delta f} \in \mathbb{C}^{M\times LF}$ (14a), and achieve the frequency- and time-frequency-DF-MUSIC.

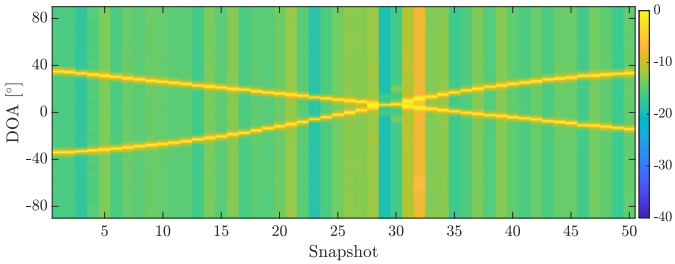

Fig. 2. $L = 1$ single snapshot DF-MUSIC (19). DOA estimation versus snapshots for dynamic DOAs.

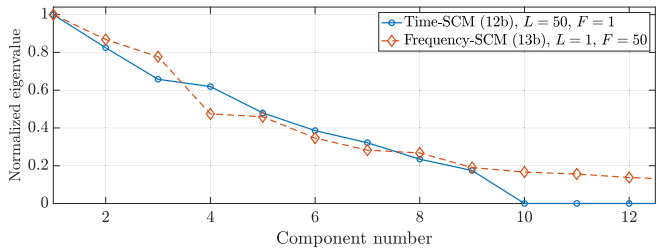

Fig. 3. Eigenvalues of DF-SCM $\mathbf{R}_{\text{DF}}$ normalized with maximum: time-(12b) (solid), frequency-(13b) (dashed), and time-frequency-DF-SCM (14b) (dash-dot). DOAs are at $[-65, -2, 3]^\circ$ and SNR $= 20$ dB.

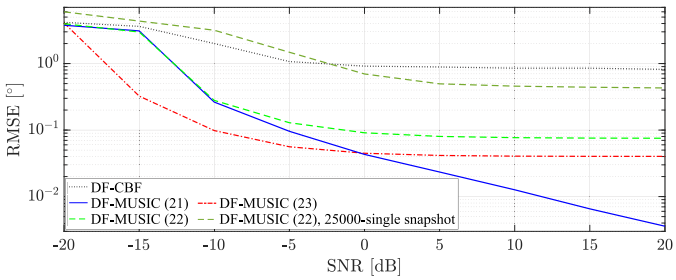

Fig. 4. RMSE versus SNR for 50 DFs and 50 snapshots. DOAs are at $[-65, -2, 3]^\circ$. Each RMSE is averaged over 500 trials.

The time-DF-MUSIC treats L samples for the DF-SCM at one DF having at least K^2 principal components (K sources and $K^2 - K$ artifacts). The method assumes that K is known, $M > K^2$, $L > K^2$, and the K^2 principal components are uncorrelated.

Joint-frequency methods consider $\mathbf{Z}_{t_l,F} \in \mathbb{C}^{M\times F}$ (13a) and $\mathbf{Z}^{\text{time-frequency}}_{\Delta f} \in \mathbb{C}^{M\times(LF)}$ (14a), and needs $F > K^2$ and $LF > K^2$, respectively. The methods assumes the principal components are uncorrelated over DFs to make DF-SCMs full rank and $M > K^2$.

V. Simulation

We consider a ULA with $M = 20$ elements, inter-sensor spacing $d = d_n = c/(2\Delta f)$, observe $L = 50$ multiple snapshot data, sound speed $c = 343$ m/s. We have uniform DF $\Delta f_i = f_i' - f_i = \Delta f = 10$ kHz, $i = 1, \ldots, F$. The lower frequencies of the DF are $F = 50$ uniformly spaced in $f_i \in [5\Delta f, 7.5\Delta f]$, and the paired upper frequencies are $f_i' = f_i + \Delta f$. The sensor spacing is half wavelength corresponding to the DF, to avoid spatial aliasing for DF processing.

The angular search grid is discretized as $[-90 : .005 : 90]^\circ$, $N = 36001$. The measurement noise (1) is modeled as IID complex Gaussian, and the lth single snapshot array signal-to-noise ratio (SNR) is SNR $= 10\log_{10}[\{\|\sum_{k=1}^{K} x_{kl,f}\mathbf{a}_f(\theta_k)\|_2^2\}/\{\|\mathbf{e}_{l,f}\|_2^2\}]$.

We first examine a scenario with two DOAs at $[-20, -15]^\circ$ with equal amplitudes but each with random phases on $[0, 2\pi)$. The frequencies are 5–8.5 times the Nyquist frequency $c/(2\,d)$, with the CBF showing strong spatial aliasing, see Fig. 1(a), and (b). Fig. 1(c), and (d) show DF-CBF (7) and DF-MUSIC (17) for each DF. DF processing overcomes spatial aliasing but shows unwanted artifact DOAs (6). The artifact DOAs vary with DFs, and averaging the spectra over DFs mitigates the artifacts, see Fig. 1(e). DF-CBF fails distinguishing the two close DOAs. DF-MUSIC has sharp peaks in the spectrum and all (18,19,20) give correct DOAs.

Fig. 2 shows the $L = 1$ single snapshot DF-MUSIC (19). The $F = 50$ DFs are as in Fig. 1. The method works well for two dynamic DOAs. Constant DF Δf enables the DF-MUSIC (19) for $F = 50$ DFs and $L = 1$ snapshot. The $L = 1$ single snapshot processing is useful for time-varying DOAs. Note that MUSIC-based methods are applicable only when DOAs are stationary over many snapshots.

Eigendecomposition of the DF-SCM $\mathbf{R}_{\text{DF}}$ is performed in Fig. 3. For time-DF-SCM (12b) at frequency $f_i = 6\Delta f$, L snapshot samples have K^2 DOAs, see (3), that are constant across time. The time-DF-SCM (12b) has K^2 principal components, which are K true DOAs, first term in (3), and $K^2 - K$ artifact DOAs, second term in (3). For frequency-DF-SCM (13b) at one time, F DF samples share the K components at the true DOAs. The $K^2 - K$ artifact DOAs varies with DF and are thus reduced by averaging.

The DOA performance is evaluated with the root mean squared error (RMSE) in Fig. 4. We examine DOAs at $[-65, -2, 3]^\circ$, SNRs from -20 to 20 dB, $L = 50$, and $F = 50$. The time-frequency-DF-MUSIC (20) achieves best RMSE at low SNRs. The frequency SCM methods (19) and (20) are biased for high SNR. The artifact DOAs (6) varying over DFs disturb the true DOAs. The frequency SCM methods integrate DF samples into a DF-SCM and obtain a noise subspace. For SNR > 0 dB, the time-DF-MUSIC (18) has lowest RMSE using joint-frequency processing using the constant DF. Averaging the single-DF spectra works better than the time-frequency DF-MUSIC.

VI. Conclusion

A DOA estimation algorithm is derived for high-frequency sources at multiple frequencies and their difference frequencies (DFs) to obtain low-frequency processing. This is spatial aliasing-free due to the DF below the aliasing frequency. The time-DF-MUSIC integrates time samples into a sample covariance matrix, obtains MUSIC spectra at each DF, and averages the spectra to estimate final DOAs. When uniform DFs are available, joint-frequency processing is available by integrating DFs into a sample covariance matrix. The frequency-DF-MUSIC works for a single-time snapshot and does not require stationary DOAs over time. The time-frequency-DF-MUSIC integrates all time and frequency, and achieves the processing gain using more data jointly.

REFERENCES

[1] W. Liu and S. Weiss, *Wideband Beamforming: Concepts and Techniques*. Hoboken, NJ, USA: Wiley, 2010.

[2] P. Gerstoft, W. S. Hodgkiss, W. A. Kuperman, H. C. Song, M. Siderius, and P. L. Nielsen, "Adaptive beamforming of a towed array during a turn," *IEEE J. Ocean. Eng.*, vol. 28, no. 1, pp. 44–54, Jan. 2003.

[3] Y. S. Yoon, L. M. Kaplan, and J. H. McClellan, "TOPS: New DOA estimator for wideband signals," *IEEE Trans. Signal Process.*, vol. 54, no. 6, pp. 1977–1989, Jun. 2006.

[4] E. D. Di Claudio, R. Parisi, and G. Jacovitti, "Space time MUSIC: Consistent signal subspace estimation for wideband sensor arrays," *IEEE Trans. Signal Process.*, vol. 66, no. 10, pp. 2685–2699, May 2018.

[5] Z. M. Liu, Z. T. Huang, and Y. Y. Zhou, "Direction-of-arrival estimation of wideband signals via covariance matrix sparse representation," *IEEE Trans. Signal Process.*, vol. 59, no. 9, pp. 4256–4270, Sep. 2011.

[6] Z. Tang, G. Blacquiere, and G. Leus, "Aliasing-free wideband beamforming using sparse signal representation," *IEEE Trans. Signal Process.*, vol. 59, no. 7, pp. 3464–3469, Jul. 2011.

[7] Z. Q. He, Z. P. Shi, L. Huang, and H. C. So, "Underdetermined DOA estimation for wideband signals using robust sparse covariance fitting," *IEEE Signal Process. Lett.*, vol. 22, no. 4, pp. 435–439, Apr. 2015.

[8] S. Nannuru, K. L. Gemba, P. Gerstoft, W. S. Hodgkiss, and C. F. Mecklenbräuker, "Sparse Bayesian learning with multiple dictionaries," *Signal Process.*, vol. 159, pp. 159–170, Jun. 2019.

[9] F. Wang, Z. Tian, G. Leus, and J. Fang, "Direction of arrival estimation of wideband sources using sparse linear arrays," *IEEE Trans. Signal Process.*, vol. 69, pp. 4444–4457, 2021.

[10] Y. Wu, M. B. Wakin, and P. Gerstoft, "Gridless DOA estimation under the multi-frequency model," in *Proc. IEEE Int. Conf. Acoust., Speech Signal Process.*, 2022, pp. 5982–5986.

[11] W. A. Gardner, "Simplification of MUSIC and ESPRIT by exploitation of cyclostationarity," *Proc. IEEE*, vol. 76, no. 7, pp. 845–847, Jul. 1988.

[12] Q. Wu and K. M. Wong, "Blind adaptive beamforming for cyclostationary signals," *IEEE Trans. Signal Process.*, vol. 44, no. 11, pp. 2757–2767, Nov. 1996.

[13] H. Yan and H. H. Fan, "Signal-selective DOA tracking for wideband cyclostationary sources," *IEEE Trans. Signal Process.*, vol. 55, no. 5, pp. 2007–2015, May. 2007.

[14] P. J. Schreier and L. L. Scharf, *Statistical Signal Processing of Complex-Valued Data: The Theory of Improper and Noncircular Signals*. Cambridge, U.K.: Cambridge Univ. Press, 2010.

[15] A. Napolitano, "Cyclostationarity: New trends and applications," *Signal Process.*, vol. 120, pp. 385–408, Mar. 2016.

[16] E. BouDaher, Y. Jia, F. Ahmad, and M. G. Amin, "Multi-frequency co-prime arrays for high-resolution direction-of-arrival estimation," *IEEE Trans. Signal Process.*, vol. 63, no. 14, pp. 3797–3808, Jul. 2015.

[17] Q. Shen, W. Liu, W. Cui, S. Wu, Y. D. Zhang, and M. G. Amin, "Focused compressive sensing for underdetermined wideband DOA estimation exploiting high-order difference coarrays," *IEEE Signal Process. Lett.*, vol. 24, no. 1, pp. 86–90, Jan. 2017.

[18] S. Qin, Y. D. Zhang, M. G. Amin, and B. Himed, "DOA estimation exploiting a uniform linear array with multiple co-prime frequencies," *Signal Process.*, vol. 130, pp. 37–46, Jan. 2017.

[19] S. Zhang, A. Ahmed, Y. D. Zhang, and S. Sun, "Enhanced DOA estimation exploiting multi-frequency sparse array," *IEEE Trans. Signal Process.*, vol. 69, pp. 5935–5946, 2021.

[20] K. Sarabandi, "Δk-radar equivalent of interferometric SAR's: A theoretical study for determination of vegetation height," *IEEE Trans. Geosci. Remote Sens.*, vol. 35, no. 5, pp. 1267–1276, Sep. 1997.

[21] S. H. Abadi, H. C. Song, and D. R. Dowling, "Broadband sparse-array blind deconvolution using frequency-difference beamforming," *J. Acoust. Soc. Amer.*, vol. 132, no. 5, pp. 3018–3029, Nov. 2012.

[22] A. S. Douglass, H. C. Song, and D. R. Dowling, "Performance comparisons of frequency-difference and conventional beamforming," *J. Acoust. Soc. Amer.*, vol. 142, no. 3, pp. 1663–1673, Sep. 2017.

[23] L. Xie, C. Sun, and J. Tian, "Deconvolved frequency-difference beamforming for a linear array," *J. Acoust. Soc. Amer.*, vol. 148, no. 6, pp. EL440–EL446, Dec. 2020.

[24] L. Yang, Y. Wang, and Y. Yang, "Aliasing-free broadband direction of arrival estimation using a frequency-difference technique," *J. Acoust. Soc. Amer.*, vol. 150, no. 6, pp. 4256–4267, Dec. 2021.

[25] B. M. Worthmann, H. C. Song, and D. R. Dowling, "High frequency source localization in a shallow ocean sound channel using frequency difference matched field processing," *J. Acoust. Soc. Amer.*, vol. 138, no. 6, pp. 3549–3562, Dec. 2015.

[26] B. M. Worthmann and D. R. Dowling, "The frequency-difference and frequency-sum acoustic-field autoproducts," *J. Acoust. Soc. Am.*, vol. 141, no. 6, pp. 4579–4590, Jun. 2017.

[27] B. M. Worthmann, H. C. Song, and D. R. Dowling, "Adaptive frequency-difference matched field processing for high frequency source localization in a noisy shallow ocean," *J. Acoust. Soc. Amer.*, vol. 141, no. 1, pp. 543–556, Jan. 2017.

[28] D. J. Geroski and B. M. Worthmann, "Frequency-difference autoproduct cross-term analysis and cancellation for improved ambiguity surface robustness," *J. Acoust. Soc. Amer.*, vol. 149, no. 2, pp. 868–884, Feb. 2021.

[29] B. D. Rao and K. V. S. Hari, "Performance analysis of root-MUSIC," *IEEE Trans. Acoust., Speech, Signal Process.*, vol. 37, no. 12, pp. 1939–1949, Dec. 1989.

[30] H. Huang, H. C. So, and A. M. Zoubir, "Off-grid direction-of-arrival estimation using second-order taylor approximation," *Signal Process.*, vol. 196, Jul. 2022, Art. no. 108513.

[31] P. Chen, Z. Chen, B. Zheng, and X. Wang, "Efficient DOA estimation method for reconfigurable intelligent surfaces aided UAV swarm," *IEEE Trans. Signal Process.*, vol. 70, pp. 743–755, 2022.

[32] X. Su, P. Hu, Z. Liu, J. Shi, and X. Li, "Deep alternating projection networks for gridless DOA estimation with nested array," *IEEE Signal Process. Lett.*, vol. 29, pp. 1589–1593, 2022.

[33] Z. Yang, P. Chen, Z. Guo, and D. Ni, "Low-cost beamforming and DOA estimation based on one-bit reconfigurable intelligent surface," *IEEE Signal Process. Lett.*, vol. 29, pp. 2397–2401, 2022.

[34] H. Groll, P. Gerstoft, M. Hofer, J. Blumenstein, T. Zemen, and C. F. Mecklenbräuker, "Scatterer identification by atomic norm minimization in vehicular mm-wave propagation channels," *IEEE Access*, vol. 10, pp. 102334–102354, 2022.

[35] S. Nannuru and P. Gerstoft, "2D beamforming on sparse arrays with sparse bayesian learning," in *Proc. IEEE Int. Conf. Acoust., Speech Signal Process.*, 2019, pp. 4355–4359.

[36] Y. Park, W. Seong, and P. Gerstoft, "Block-sparse two-dimensional off-grid beamforming with arbitrary planar array geometry," *J. Acoust. Soc. Amer.*, vol. 147, no. 4, pp. 2184–2191, Apr. 2020.

[37] F. Wen, G. Gui, H. Gacanin, and H. Sari, "Compressive sampling framework for 2D-DOA and polarization estimation in mmWave polarized massive MIMO systems," *IEEE Trans. Wirel. Commun.*, early access, 01 Nov, 2022, doi: 10.1109/TWC.2022.3215965.

[38] D. Kim, W. Seong, Y. Choo, and J. H. Lee, "Localization of incipient tip vortex cavitation using ray based matched field inversion method," *J. Sound Vib.*, vol. 354, pp. 34–46, Oct. 2015.

[39] J. H. Lee, "Acoustic localization of incipient cavitation in marine propeller using greedy-type compressive sensing," *Ocean Eng.*, vol. 197, Feb. 2020, Art. no. 106894.

[40] C. Evers et al.,, "The LOCATA challenge: Acoustic source localization and tracking," *IEEE/ACM Trans. Audio, Speech, Lang. Process.*, vol. 28, pp. 1620–1643, 2020.

[41] M. Wagner, Y. Park, and P. Gerstoft, "Gridless DOA estimation and root-MUSIC for non-uniform linear arrays," *IEEE Trans. Signal Process.*, vol. 69, pp. 2144–2157, 2021.

[42] Y. Park and P. Gerstoft, "Gridless sparse covariance-based beamforming via alternating projections including co-prime arrays," *J. Acoust. Soc. Amer.*, vol. 151, no. 6, pp. 3828–3837, Jun. 2022.

[43] B. Kilic, A. Güngör, M. Kalfa, and O. Arıkan, "Adaptive measurement matrix design in direction of arrival estimation," *IEEE Trans. Signal Process.*, vol. 70, pp. 4742–4756, 2022.

[44] L. Zhou, K. Ye, J. Qi, and H. Sun, "DOA estimation based on pseudo-noise subspace for relocating enhanced nested array," *IEEE Signal Process. Lett.*, vol. 29, pp. 1858–1862, 2022.

[45] S. Qin, Y. D. Zhang, and M. G. Amin, "Generalized coprime array configurations for direction-of-arrival estimation," *IEEE Trans. Signal Process.*, vol. 63, no. 6, pp. 1377–1390, Mar. 2015.

[46] P. Kulkarni and P. P. Vaidyanathan, "Non-integer arrays for array signal processing," *IEEE Trans. Signal Process.*, vol. 70, pp. 5457–5472, 2022.

[47] A. G. Raj and J. H. McClellan, "Single snapshot super-resolution DOA estimation for arbitrary array geometries," *IEEE Signal Process. Lett.*, vol. 26, no. 1, pp. 119–123, 2018.

[48] Y. Wang, Y. Zhang, Z. Tian, G. Leus, and G. Zhang, "Super-resolution channel estimation for arbitrary arrays in hybrid millimeter-wave massive MIMO systems," *IEEE J. Sel. Topics Signal Process.*, vol. 13, no. 5, pp. 947–960, Sep. 2019.

[49] P. Gerstoft, R. Menon, W. S. Hodgkiss, and C. F. Mecklenbräuker, "Eigenvalues of the sample covariance matrix for a towed array," *J. Acoust. Soc. Amer.*, vol. 132, no. 4, pp. 2388–2396, Oct. 2012.